Journal of Visualization, Vol. 12, No. 3 (2009) 241-250

Regular Paper

Wall-PIV as a Near Wall Flow Validation Tool for CFD:

Application in a Pathologic Vessel Enlargement (Aneurysm)

Goubergrits, L.*[1], Weber, S.*[1], Petz, Ch.*[2], Hege, H-Ch.*[2], Spuler, A.*[3], Poethke, J.*[1], Berthe, A.*[1], and Kertzscher, U.*[1]

*1 Biofluid Mechanics Laboratory, Charité - Universitätsmedizin Berlin, Germany.
E-mail: biofluidmechanik@charite.de
*2 Visualization and Data Analysis, Zuse-Institute Berlin, Germany.
*3 Neurosurgery Department, Helios Hospital Berlin-Buch, Germany.

Received 12 April 2008
Revised 4 February 2009

Abstract: Flow visualization of a near wall flow is of great importance in the field of biofluid mechanics in general and for studies of pathologic vessel enlargements (aneurysms) particularly. Wall shear stress (WSS) is one of the important hemodynamic parameters implicated in aneurysm growth and rupture. The WSS distributions in anatomically realistic vessel models are normally investigated by computational fluid dynamics (CFD). However, the results of CFD flow studies should be validated. The recently proposed Wall-PIV method was first applied in an enlarged transparent model of a cerebri anterior artery terminal aneurysm made of silicon rubber. This new method, called Wall-PIV, allows the investigation of a flow adjacent to transparent surfaces with two finite radii of curvature (vaulted walls). Using an optical method which allows the observation of particles up to a predefined depth enables the visualization solely of the boundary layer flow. This is accomplished by adding a specific molecular dye to the fluid which absorbs the monochromatic light used to illuminate the region of observation. The results of the Wall-PIV flow visualization were qualitatively compared with the results of the CFD flow simulation under steady flow conditions. The CFD study was performed using the program FLUENT®. The results of the CFD simulation were visualized using the line integral convolution (LIC) method with a visualization tool from AMIRA®. The comparison found a very good agreement between experimental and numerical results.

Keywords: PIV, Wall Shear Flow, Molecular Dye, LIC Visualization, CFD.

1. Introduction

The assessment and visualization of flow along a vaulted wall (wall with two finite main radii of curvature) is of special interest in biofluid mechanics. The flow adjacent to the wall of natural vessels or artificial organs (blood pumps or heart valves) is interesting since atherosclerotic wall alterations or thrombus formations develop here (e.g., Asakura et al., 1990). These pathologic processes were proved to be related with the hemodynamic parameter – wall shear stress (e.g., Malek et al., 1999, e.g., Affeld et al., 2004).

Cerebral aneurysms are pathological vessel enlargements in the brain circulation. Aneurysms are potentially life threatening. The main risk inherent to aneurysms is rupture. Growth rate, risk of the rupture and the location of the rupture site depend on the mechanical property of the vessel wall (e.g., Austin et al., 1989) which we cannot assess directly in a patient. However, composition and

properties of the aneurysmal wall are influenced by wall shear stress (WSS) and by wall stress, which are locally distributed parameters. A large body of evidence demonstrates the influence of WSS on vascular endothelial cells as well as on vascular smooth muscle cells (e.g., Griffith, 2002, e.g., Resnick et al., 2003), resulting in different events such as flow mediated vasodilatation, atherosclerosis and vascular remodeling. Therefore, the prediction of WSS based on the anatomically realistic three-dimensional (3D) reconstruction of the vessel geometry may help to foresee the natural development of an incidentally detected aneurysm in an individual patient and facilitate treatment decisions.

Current measurement methods have problems assessing the flow along vaulted walls and hence WSS distributions in complex geometries, such as of aneurysms (see fig. 1). Normally, the WSS is assessed by computational fluid dynamics (CFD). With the recent development of 3D medical imaging it is now possible to reliably simulate blood flow in anatomically realistic vessel geometries. However, the CFD simulations in complex geometries should be validated. This study presents a qualitative comparison between experimental and numerical near wall flow visualization in an enlarged transparent silicon model of an aneurysm. The experimental near wall flow visualization was done using a recently proposed Wall-PIV technique (e.g., Debaene et al., 2005, e.g., Kertzscher et al., 2008).

2. Materials and Methods

2.1 Reconstruction of the aneurysm geometry

For surgical planning, a standard computed tomography (CT) angiography was performed in the Helios Hospital, Berlin-Buch. The CT resulted in slices of 2 mm thickness with 1 mm distance in a 512x512 pixel matrix with a 16-bit gray scale. These raw data were used for the three-dimensional reconstruction of a trifurcation aneurysm of the cerebri anterior artery. By means of the image processing program AMIRA® (Mercury Computer Systems, Chelmsford, USA), a geometrical reconstruction of the aneurysm was performed. In order to extract the aneurysm, thresholding and semi-automatic image segmentation was performed for each slice. Then, all slices containing the aneurysm contour were stacked up to construct a 3D-isosurface of the aneurysm. After applying smoothing algorithms, a solid geometric model was constructed and a stereo-lithographic (STL) data file was created (see fig. 1, left). At the inlet of the computer model a cube was generated. This cube would serve later in the experimental model for the three-dimensional positioning of the model in space in order to allow an exact comparison between experimental results and CFD flow simulation data. The edges of the cube are aligned with xyz-directions of our coordinate system. The aneurysm surface can be virtually divided into two approximated half-spheres: the half-sphere between branches 1 and 2 (HS1), which is visible in figure 1 left, and the opposite half-sphere located between

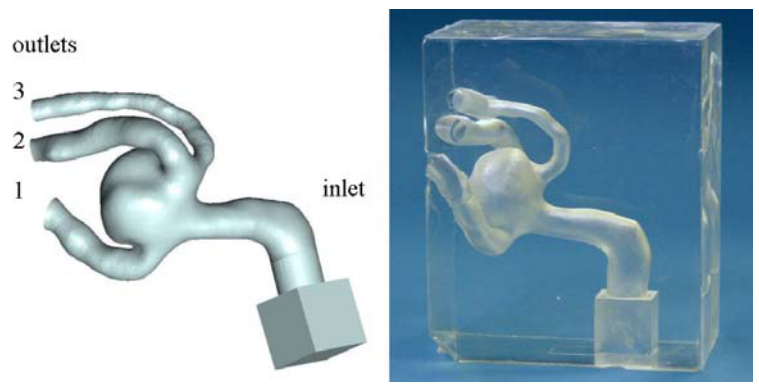

Fig. 1. Left: Computer model of the reconstructed aneurysm used in this study. Right: Threefold enlarged transparent silicone model of the reconstructed aneurysm which was fabricated from the STL data file shown on the left.

branches 1 and 3 (HS2).

Using the above mentioned STL data file, a threefold upscale aneurysm model was fabricated using the rapid prototyping technique with a resolution of 0.1 mm including a manual finish in order to produce a rubber mold. The mold was filled with Wood's metal, resulting in a cast. Wood's metal is a fusible eutectic alloy of bismuth, lead, tin, and cadmium with the following percentages by weight: 50% Bi, 26.7% Pb, 13.3% Sn, 10% Cd. Wood's metal liquefies at approximately 70 °C. Wood's cast was then used to fabricate a nearly rigid transparent silicone block model (see fig. 1, right). We used the two-component silicone rubber ELASTOSIL RT 601 (Wacker-Chemie GmbH, Munich, Germany) for the model fabrication. The refraction index of the silicone rubber is n = 1.4. The model was generated by filling the box containing the Wood's cast with the liquid silicone in a vacuum casting machine in order to remove air bubbles. After the silicone hardened, the cast was boiled out in a water tank. The size of the silicone block is 55 mm x 95 mm x 115 mm. The size of the aneurysm geometry in the silicone block is 40 mm x 65 mm x 60 mm. The inner duct diameter was equal to the aneurysm model inlet diameter of D = 14 mm.

2.2 Wall-PIV

This chapter gives an overview of the Wall-PIV method. The method allows potentially the evaluation of all three velocity components of flows within the range of hundred micrometers or less adjoining a transparent vaulted wall – walls with two finite radii of curvature. The denomination Wall-PIV is used because of the similarity of the proposed technique to Particle Image Velocimetry. The basic principles of the PIV technique are well described by Adrian (e.g., Adrian, 1991).

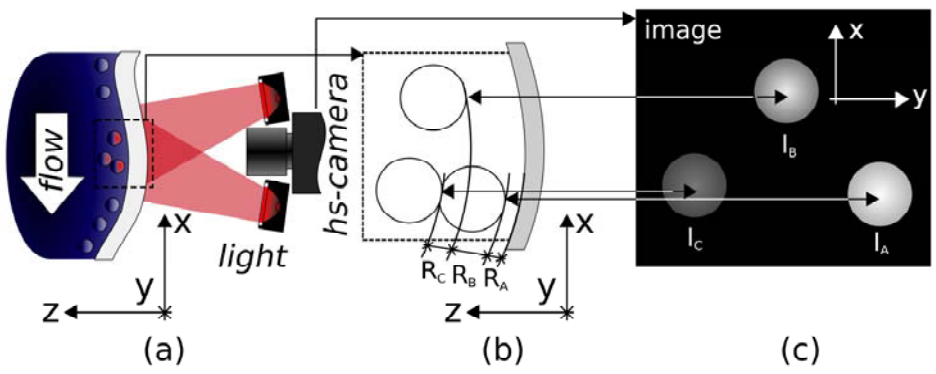

Fig. 2. Illustration of the Wall-PIV method: (a) Sketch of part of the fluid flow and the apparatus used, showing the near wall illuminated region of the fluid and the tracers. (b) Detail of the rectangular region indicated in part (a), showing the distances of the particles A, B, and C to the wall. (c) Image recorded by the camera with the corresponding particle intensities I_A, I_B, and I_C.

Analogous to PIV, in Wall-PIV reflecting particles are added to the fluid as tracers and are recorded with a digital camera. The first key difference is the illumination of the flow, which is not realized with a laser light sheet (which could at most be curved, but not vaulted) but with diffuse monochromatic light. The source of the diffuse light is placed outside of the flow model next to the camera as is shown in figure 2. The limitation of the field of view to the region adjoining the model wall is realized by adding a molecular dye to the fluid, a second key difference to standard PIV. The dye causes the absorption of the light, allowing the depth of penetration to be adjusted by varying either the incoming light intensity I_0 or the concentration of the dye c.

The third component of the observed particles' positions can be obtained by the brightness of the particles, which is expressed through their grey values. In the observed region, a particle close to the wall has less absorbing fluid between its surface and the wall than a particle which is farther away from the wall. This means that the intensity of the reflected light from the particle closer to the wall is higher than that of the particle farther away from the wall, resulting in the brighter

appearance of the particle which is closer (see fig. 2 b and c). Therefore, the grey values of the observed particles imply information regarding their distance to the wall. Analytically, the relationship between the brightness of the particles and their distance to the wall can be derived from Beer-Lambert's law:

$$I = I_p \cdot e^{-\varepsilon \cdot c \cdot R} = I_0 \cdot e^{-2 \cdot \varepsilon \cdot c \cdot R} \tag{1}$$

In equation 1, ε is the molar absorption coefficient of the dyed fluid and c is the concentration of the dye. I_0 is the light intensity generated by a light source; I_p is the reduced light intensity that reaches a particle located at the distance of R from the wall surface; and I is the resulting intensity transmitted to the sensor of the camera. The recorded grey value is proportional to the given intensity if the difference in the light intensity caused by passing through the transparent wall and the region between wall and camera is neglected. Partial reflection of the light on the particle's surface and other optical effects can be taken into account by calibration.

Since all three components of the particles' positions are known, all three velocity components may be computed. As in PIV, the movement of the particles can be used to reconstruct the velocity field in the near wall region. Therefore, various different evaluation techniques, such as cross-correlation, particle tracking and optical flow (OF), are applicable. These standard evaluation techniques allow the reconstruction of 2D-flow-fields adjoining the vaulted wall. Our experience revealed a mean particle concentration between 4 and 12 particles per 32x32 pixel areas. A relative low particle concentration in a near wall region of laminar flows is caused by a particle-wall interaction with a well known radial migration of particles (e.g., Michaelides, 2003). The optimal particle density for the PIV technique was found to be 15 particles per 32x32 pixel interrogation area (e.g., Keane and Adrian, 1990). In comparison, PTV algorithms allow the tracking of approximately 1000 – 1500 particles (e.g., Netzsch and Jähne, 1995) or up to 5 vectors per 32x32 pixel interrogation area in combined PIV/PTV algorithms (e.g., Tan and Hart, 2002), which is significantly lower than the number of particles in our images. This is why we decided to use the OF algorithm for the assessment of the 3D-3C near wall flow field. The basic principle of the OF is well described by Horn and Schunck (e.g., Horn and Schunck, 1981). The development of the algorithms for this 3D-3C flow analysis is now being evolved by the Interdisciplinary Centre for Scientific Computing (IWR) at the University of Heidelberg (e.g., Jehle et al., 2006). This includes an implementation of Beer-Lambert's law into the right part of the basic equation of the OF – BCCE (brightness change constraint equation) - as well as further verification and validation of the algorithms with single particle setups. In spite of the fact that the OF algorithm is under development, the Wall-PIV technique may be used now for flow visualization of the near wall path lines. The experimental setup and the Wall-PIV visualization are described in the next chapter.

2.3 Experimental setup

Sequences of images of the near wall flow in the aneurysm model are acquired using the Wall-PIV technique. The reconstruction and fabrication procedures of the enlarged silicon model (see fig. 1 right) were described in chapter 2.1. The steady laminar flow with the Reynolds number Re = 300 was based on the dynamic viscosity of blood with $\nu = 0.0035$ Pa·s, the inlet diameter of the aneurysm model D = 14 mm and a flow rate of 600 ml/min. The flow rate in the model was calculated based on the Reynolds similarity for the threefold enlarged model and the known mean flow rate of the inlet artery (internal carotid artery) of 200 ml/min in humans according to literary data (e.g., Scheel et al., 2000, e.g., Kato et al., 2002). The flow was generated using a self-developed computer-controlled piston pump. We employed a microprocessor (Rabbit Semiconductor, Davis, USA) controlled piston pump with a fluid volume of 1 l. The pump driving DC motor (Maxonmotor, Sachseln, Swiss) was actuated by the Faulhaber motion controller MCDC3006S. Pump housing and piston were made from polyoxymethylene. The guide rings were made of Teflon and the single acting seal/scraper Turcon Variseal (Trelleborg Sealing Solutions, Stuttgart, Germany) was used for the pumping of

fluids containing damageable tracers.

The test fluid was a glycerine/distilled water mixture (37.5% of the 99.5% pure glycerine), which has the same refractive index as the silicone model (n=1.4), with the added 0.3 g/l molecular dye Patent Blue V (Schumann and Son, Germany). The absorption of the Patent Blue V dye is optimal for a wavelength of 639 nm, which is the maximum in the spectral sensitivity of the used high speed camera Fastcam-Super 10K (Photron, Tokyo, Japan). The measured density of the test fluid was 1.1038 g/cm^3. The experimentally measured kinematic viscosity of the test fluid was $3.47 \cdot 10^{-6}$ m^2/s at the temperature T = 24°C. The kinematic viscosity of the mixture was measured with the Cannon-Fenske-Routineviscosimeter type 50101/0a from the firm SCHOTT with an inner diameter of d = 1.01 mm. The measurement accuracy was 1%. In order to generate a well defined velocity inlet profile at the model inlet, we connected the silicone model to the pump with a rigid duct with an inner diameter D = 14 mm and a length L = 650 mm. This length was enough to generate a fully developed parabolic inlet velocity profile as calculated by equation 2:

$$L = D \cdot 0.065 \cdot \mathrm{Re} \tag{2}$$

The test fluid was seeded with Conduct-o-fil AGSL 150-30 TRD particles with a density of 1.1 g/cm^3 fabricated by Potters Industries Inc. The particles were sieved to obtain nearly monodisperse particles with diameters between 71 μm and 75 μm. The three outlets of the model were connected to the three separate collecting reservoirs which were also used to measure volumetrically the flow rate ratio.

The model was illuminated by a set of 56 Luxeon Light emitting diodes (LED) (Philips Lumileds Lighting, USA), which were powered by a power supply with 3 W and emitted the wave length λ = 627 nm (red). All LED's were equally distributed in eight rows covering an area of 130 mm x 110 mm and were located near the camera. According to our experimentally obtained calibration curve, the particles were seen up to a depth of 140 μm. The camera was positioned at a distance of 710 mm. With the used 1.8 mm or 2.8 mm apertures, the resulting depth of focus was between 21 mm and 28 mm.

As mentioned above, we used the high speed camera Fastcam-Super 10K with a resolution of 512x480 pixel and 250 frames per second. A camera memory consisting of 255 Mb allowed us to acquire maximally 546 images during a period of 2.184 s. Based on the sequences of 546 images, max-min images were generated. A max-min image is obtained by subtracting the min-image from the max-image. The max-image is generated by calculating the maximal grey values for each pixel of the image over a defined sequence, whereas the min-image is generated by the calculation of the minimal grey values. The resulting max-min image is well suited for path line visualization (fig. 3).

2.4 CFD

The numerical solution of steady Navier-Stokes equations for momentum and mass conservation governing fluid motion under defined boundary conditions were solved by a control volume finite element method implemented in FLUENT 6® (ANSYS-Fluent Inc., Lebanon, USA). The numerical simulation was performed with the model geometry scaled to the size of the experimental model.

For finite element numerical simulation the vessel volume had to be represented by a mesh grid. The transformation of the volume data into a mesh was performed by means of the pre-processor Gambit® (ANSYS-Fluent Inc., Lebanon, USA). The surfaces of the vessels were triangulated with a node distance between 0.3 and 0.6 mm (1:20 of the mean vessel diameter D). Based on this surface mesh, a grid composed of tetrahedral elements was generated in the reconstructed vessels. The total number of nodes exceeded 35,000. The number of the surface elements (triangles) was approximately 50,000. Recently, some detailed studies were performed regarding the mesh resolution required to appropriately simulate the blood flow in coronary arteries using finite element methods (e.g. Prakash and Ethier, 2001). The authors found that a high mesh resolution near the walls was needed to get accurate values of WSS. Based on these studies, we

generated a mesh which was refined in the near wall region. A boundary layer was generated consisting of three rows with a growth factor of 1.2 (ratio between two consecutive layers near the wall) and a total depth of 0.7 mm. The quality of the generated mesh grid was assessed using different approaches. The maximal skew of their distribution was, for example, below 0.75, which is fully satisfactory. The resulting number of grid volume elements was approximately 700,000 cells (prisms and tetrahedrons).

A steady laminar flow was simulated presuming rigid motionless walls. A no-slip condition was assumed at the wall. The pressure value was not imposed at the outlet. The test fluid used in the experiments was modeled as a Newtonian fluid with a kinematic viscosity of $3.47 \cdot 10^{-6}$ m²/s at a room temperature of 24°C. A second order discretization scheme and a SIMPLEC model for pressure flow coupling were used. A parabolic inlet velocity profile was generated using a user defined function (UDF) which was implemented in FLUENT. An experimentally measured flow rate relation of 29%/34%/37% between outlets 1, 2 and 3 (see fig. 1 left) was assumed between the three outlet vessels of the aneurysm trifurcation. The mean flow rate at the inlet was the same as in the experiments. According to literary data, the mean inlet velocity is then equal to the 0.3 m/s. The convergence criteria for relative errors in velocity components and pressure were set to 10^{-4}.

For the validation of the experimentally observed near wall flow, the WSS vector field of the simulated flow is used. The WSS vector field is calculated with three velocity components at the near wall cell centre divided by a distance between a cell centre and a cell face defining the wall boundary. Hence, WSS vector field corresponds with a near wall velocity vector field. It is visualised with the line integral convolution (LIC) method (Stalling, 1995). The LIC technique shows the streamlines of the WSS vector field visually dense, this is achieved by smearing a white-noise pattern along the directions of the vector field. As shown in fig. 5, the resulting pattern on the surface clearly reveals important flow phenomena such as recirculations, stagnations and saddles. The LIC visualization was realised using the software AMIRA® (Mercury Computer Systems, Chelmsford, USA).

3. Results

3.1 CFD

Figures 3 and 4 show three-dimensional complex flow field in the cerebry anterior aneurysm visualized by path lines. Path lines were calculated reversely from the three outlet branches and separated by three colors: green – outlet 1, blue – outlet 2, red – outlet 3 (see fig. 1). These path lines form three separated flow streams. Due to the asymmetric aneurysm formation relatively to the inlet branch, the main blood stream enters the aneurysm along the wall HS1 (see section 2.1) turns by 180° at the aneurysm dome and flows mainly along the wall HS2 to the three outflow branches. The turned stream meets against the inlet flow stream that forms a saddle critical point (see fig. 6, (c)) at the HS2. There is a strong separation between flow stream of the outflow branch 1 and the outflow branches 2 and 3. These streams are clearly separated that is visible by divergent surface LIC streamlines at HS1 (see fig. 5 right). The major part of the green stream leaves the aneurysm through the outlet branch 1 after a one rotation in the aneurysm (see fig. 4 left) and forms an attracting focus at the vessel wall (see fig. 6, (d)). The red stream, which leaves the aneurysm through the outlet 3 flows mainly along the aneurysm wall and forms an S-shaped stream (see fig. 4 right). The red stream forms also a vortex at the bifurcation apex of the branches 2 and 3 (see fig. 3 right). The blue stream (see fig. 4 middle) generates a strong vortex in the aneurysm filling the major part of the aneurysm volume.

Figure 5 (left) shows the main result of the numerical flow simulation in the cerebry anterior aneurysm – the WSS distribution. Regions of low and high WSS values are found. Based on the WSS vector field the LIC visualization of the near wall flow field was generated. Figure 5 (right) shows LIC image calculated with a surface WSS vector field, whose magnitude distribution is shown in figure 5 (left). The LIC visualization shows the same flow features as were found by the path line

visualization based on the Wall-PIV technique (see fig. 6 up). Figure 6 down shows LIC images corresponding to the max-min images.

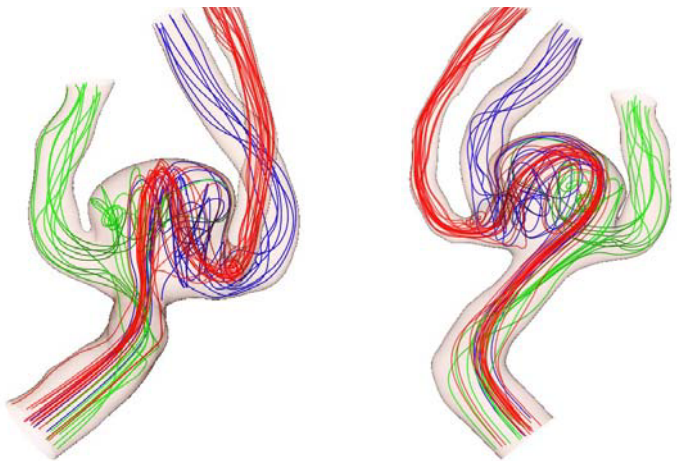

Fig. 3. Flow field in the aneurysm visualized by path lines separated in three colors related to the three outflow branches. Two view directions are shown for better 3D-representation of the complex flow field.

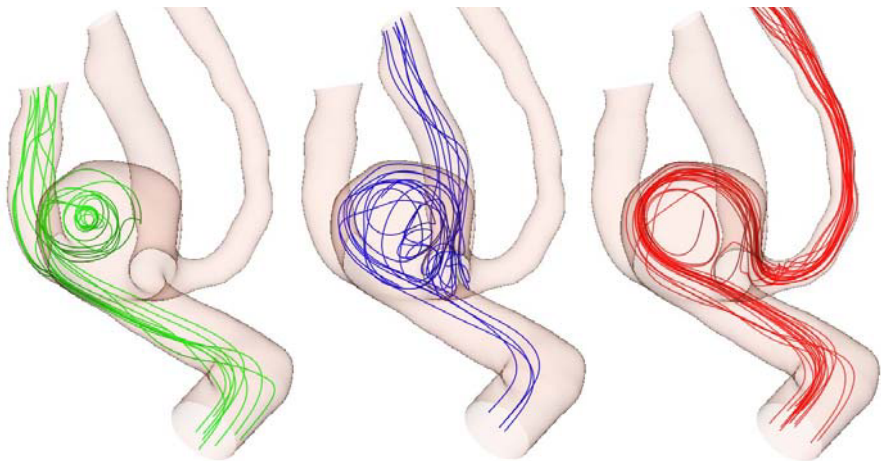

Fig. 4. Flow field in the aneurysm visualized by path lines separated in three colors related to the three outflow branches (green – outlet 1, blue – outlet 2, red – outlet 3). Three separated branch streams are shown.

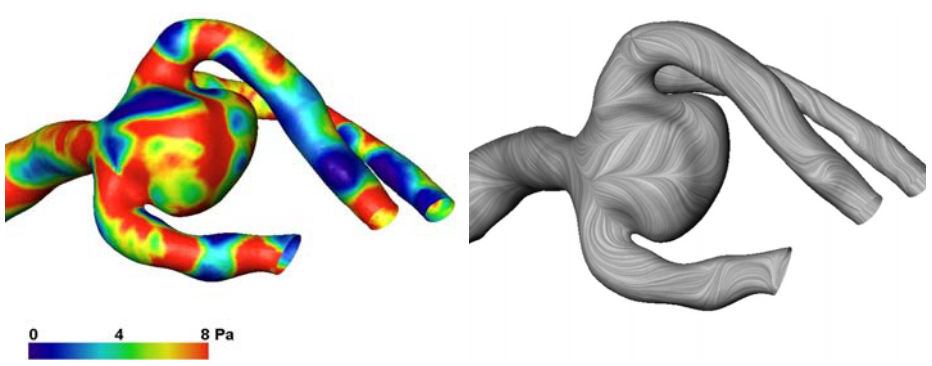

Fig. 5. Left: WSS magnitude distribution. Red also indicates all WSS values higher than 8.0 Pa. Right: LIC image of the corresponding WSS surface vector field.

3.2 Wall-PIV

Figure 6 shows four max-min images of the investigated model of the cerebry anterior aneurysm. Two left images (see fig. 6, (a) and (b)) show HS1 surface of the aneurysm, whereas two right images (see fig. 6, (c) and (d)) show HS2 surface. The resulting path lines show a very complex near wall flow field including critical points (stagnation and saddle points) with zero wall shear stress and lines with diverging and converging flows. The near wall flow is formed by three flow streams, which were described in section 3.1. In some regions the path lines are not visible. This is caused by the restricted depth of focus (28 mm).

Figure 6 shows a correspondence between the near wall flow fields calculated by CFD and assessed by the Wall-PIV technique. The characteristic features of the flow pattern are very similar for LIC and Wall-PIV path lines: Divergent lines without any critical points at the aneurysm surface HS1 and divergent lines at the bifurcation of the outlet branch 1 in the left images (see fig. 6, (a)), double critical point (saddle and stagnation) found in the outlet branch 2 and marked by a circle in the second image from left and divergent lines visible between outlet branches 2 and 3 (see fig. 6, (b)). Finally, two critical points (saddle and attracting focus), which are marked by circles in the two right images (see fig. 6, (c) and (d)), show also a good agreement. Unfortunately, the inflow of the aneurysm is out of focus in the wall-PIV results (see fig. 6, (c)). Therefore, only the stream from the aneurysm dome can be clearly identified. Due to the low particle density at the critical points, they are not well represented but still visible. The low particle density at critical points, for example, makes difficult a separation of the double critical point marked in the fig. 6, (b). This problem, however, can be solved by a use of camera with more memory storage than the 546 images allowed by the used camera.

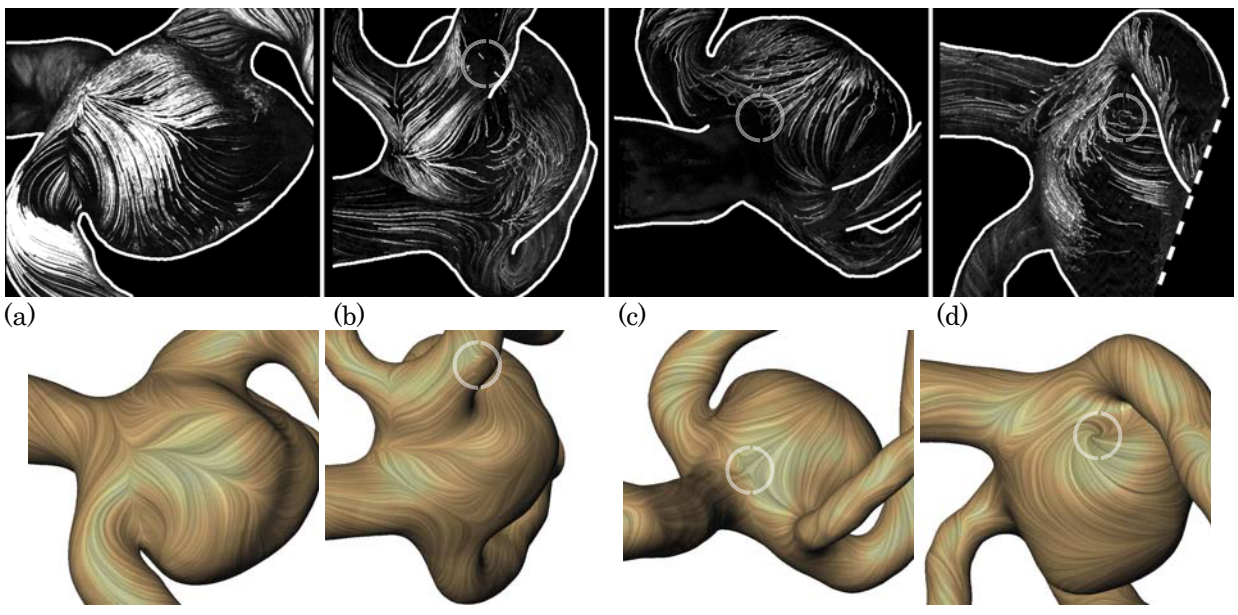

Fig. 6. Four upper images show min-max images of the near wall flow in the cerebry anterior aneurysm model acquired from different directions. Four down images show LIC images. Two left images show HS1 wall of the aneurysm. Two right images show mainly HS2 wall. Circles mark the critical points.

4. Discussion and Conclusion

The near wall flow in the transparent silicone model of the cerebry anterior aneurysm was visualized using max-min images resulting from images acquired with the Wall-PIV technique. The flow in the same geometry was then calculated numerically using the CFD software FLUENT and visualized using the LIC technique implemented in the software AMIRA. The comparison between experimental and numerical results found a very good agreement between the path lines visualized

by Wall-PIV and the WSS vector field visualized on the surface by LIC. The good agreement was found both for divergent stream lines and location of critical points. This study was performed under steady flow conditions. Experiments under pulsatile flow condition are planned. However, pulsatile flow simulations that we performed found an error below 3 % between steady and time-averaged WSS field.

The results of this study showed the ability of the novel technique to visualize the near wall flow at vaulted walls and the ability of the Wall-PIV visualization technique to serve as a validation tool for CFD results. Note that this validation method is similar to the oil film visualization, which is also used for the validation of CFD results (e.g., Suzuki and Arakawa, 2006). After the development of the OF algorithm for the 3D-3C near wall velocity vector field, the Wall-PIV technique will be applied for quantitative validation of the WSS fields calculated by CFD. This step needs also an accurate calibration and validation of the particle-wall distance definition. In our earlier published paper describing the development of the Wall-PIV technique a quantitative difference between experimentally measured and with CFD calculated WSS values was between 5 and 15 % depending on the complexity of the geometry and flow field (e.g., Debaene et al., 2005). The use of new, significantly smaller particles (diameter of old particles was about 340 μm) and a use of OF algorithm instead of cross-correlation is expected to improve the proposed technique.

References

Malek, A.M., Alper, S.L. and Izumu, S., Hemodynamic shear stress and its role in atherosclerosis, J. Am. Med. Assoc., 282 (1999), 2035-2042.

Affeld, K., Goubergrits, L., Kertzscher, U., Gadischke, J. and Reininger, A., Mathematical model of platelet deposition under flow conditions, Int J Artif Organs, 27-8 (2004), 699-708.

Austin, G.M., Schievink, W. and Williams, R., Controlled pressure-volume factors in the enlarged of intracranial aneurysms, Neurosurgery 24-5 (1989), 722-730.

Griffith, T.M., Endothelial control of vascular tone by nitric oxide and gap junctions: A hemodynamic perspective, Biorheology 39 (2002), 307-318.

Resnick, N., Einav, S., Chen-Konak, L., Zilberman, M., Yahav, H. and Shay-Salit, A., Hemodynamic forces as stimulus for arteriogenesis, Endothelium 10-4-5 (2003), 197-206.

Debaene, P., Kertzscher, U., Goubergrits, L. and Affeld, K., Visualization of a wall shear flow: Development of a new Particle Image Interrogation method, Journal of Visualization 8-4 (2005), 305-314.

Kertzscher, U., Berthe, A., Goubergrits, L., Affeld, K., Particle image velocimetry of a flow at a vaulted wall. Proc IMechE, Part H: Journal of Engineering in Medicine 222-4 (2008), 465-473.

Prakash, S. and Ethier, C.R., Requirements for mesh resolution in 3-D computational hemodynamics, Journal of Biomedical Engineering 123 (2001), 26-38.

Kato, T., Indo, T., Yoshida, E., Iwasaki, Y., Sone, M. and Sobue G., Contrast-Enhanced 2D Cine Phase MR Angiography for Measurement of Basilar Artery Blood Flow in Posterior Circulation Ischemia, Am. J. Neuroradiol. 23 (2002), 1346–1351.

Scheel, P., Ruge, Ch., Petruch, U.R. and Schöning M., Color Duplex Measurement of Cerebral Blood Flow Volume in Healthy Adults, Stroke 31 (2000), 147-150.

Adrian, R. J., Particle-imaging techniques for experimental fluid mechanics, Ann. Rev. Fluid Mech., 23 (1991), 261-268.

Jehle, M., Kertscher, U. and Jähne, B., Direct estimation of the wall shear rate using parametric motion models in 3D. In: Lecture Notes in Computer Science – Pattern Recognition, Springer, Berlin, Germany, 4174 (2006), 434–443.

Keane, R.D. and Adrian, R.J., Optimization of particle image velocimeters. Part I: Double-pulsed systems, Meas. Sci. Technol. 1 (1990), 1202-1215.

Michaelides, E.E., Hydrodynamic force and heat/mass transfer from particles, bubbles, and drops – The Freeman Scholar Lercture, J. Fluids Eng – T ASME 125 (2003), 209-238.

Netzsch, T. and Jähne, B., A high performance system for 3-dimensional particle tracking velocimetry in turbulent flow research using image sequences, Proc. of ISPRS Intercommission, Workshop 'From Pixels to Sequences', in International Archives of Photogram and Remote Sensing 30 (1995), Part 5W1.

Tan, S. and Hart, D.P., A novel particle displacement measurement method using optical diffraction, Measurement Science and Technology 13 (2002), 1014-1019.

Horn, B. and Schunck, B., Determining optical flow, Artificial Intelligence 17 (1981), 185–204.

Jehle, M., Kertscher, U. and Jähne, B., Direct estimation of the wall shear rate using parametric motion models in 3D, In: Lecture Notes in Computer Science – Pattern Recognition 4174 (2006), 434–443.

Stalling, D. and Hege, H.-Ch., Fast and resolution independent line integral convolution, In: Proceedings of the 22nd annual conference on computer graphics and interactive techniques (1995), 249–256.

Suzuki, M. and Arakawa, C., Flow on blades of wells turbine for wave power generation, Journal of Visualization 9-1 (2006), 83-90.

Author Profile

Leonid Goubergrits: He received his MSc (Physics) in Fluid Mechanics in 1993 from the Moscow Institute of Physics and Technology, Department of the Aeromechanics and Flying Machines, Russia Federation. He also received his doctorate in Engineering in 2000 from the Technische Universität Berlin. Since 1996 Leonid Goubergrits works at the Biofluid Mechanics Laboratory, Charité - Universitätsmedizin Berlin, Germany as a research assistant. He also teaches Biofluid Mechanics at the Technische Universität Berlin. His research interests are quantitative visualization, PIV, CFD, flow optimization of the artificial organs and flow analysis of the blood flow in native vessels and artificial organs including modeling of the blood damage.

Sarah Weber: She studied Physical Engineering at the Technische Universität Berlin. Currently, she is working at the Biofluid Mechanics Laboratory, Charité - Universitätsmedizin Berlin, Germany as a research assistant. Her research interests are quantitative visualization, PIV, CFD and analysis of the blood flow in native vessels and especially in capillaries that includes the multiphase blood modeling. The study presented here is a part of her diploma thesis.

Christoph Petz: He received his diploma in computer science in 2003 from the University of Marburg, Germany. He wrote his diploma thesis at the Max-Planck-Institut für Informatik. Currently, he works at the Konrad-Zuse-Institute Berlin (ZIB) as a researcher at the Scientific Visualization group. His research interests are hardware-based rendering and volume visualization.

Andreas Spuler: He studied Medicine in Würzburg, Vienna, and Zurich. He received his doctorate in Medicine from the Ludwig-Maximilians University Munich in 1989. As a postdoctoral fellow he worked at the Institute of Neurophysiology in Munich and at the Brain Research Institute in Zurich. He did his residency in neurosurgery at the University Hospital Munich and a neurosurgical fellowship at the Mayo Clinic Rochester 1996/1997. Since 1999 he is vice chairman of the neurosurgical department of the Helios Klinikum Berlin-Buch. His research interest is focused on neurovascular disorders, their pathophysiology and treatment.

Andre Berthe: He studied Chemical and Power Engineering as well as Environmental engineering at the Technical University of Berlin and the École des Mines des Saint-Etiènne. Receiving three diplomas in 2005 and 2006 he works at the Biofluid Mechanics Laboratory, Charité – Universitätsmedizin Berlin as research assistant and prepare his doctor thesis. His research interests are quantitative visualization, PIV, data treatment and the development of optical measurement techniques. Postgraduate student at the Technische Universität of Berlin.

Hans-Christian Hege: He studied physics, mathematics and philosophy at Free University Berlin. Hon. Prof. H.-Ch. Hege is a head of the Department Visualization and Data Analysis in the Division Scientific Computing of the Zuse-Institute Berlin, which he started in 1991. His research interests are data visualization, image analysis and virtual laboratories for life sciences, natural sciences and engineering. His major interest is in design and development of effective techniques for visual data analysis.

Jens Poethke: He received his diploma in Physical Engineering from the Technische Universität Berlin in 2007. Since 2007 Jens Poethke works at Biofluid Mechanics Laboratory, Charité - Universitätsmedizin Berlin as research assistant and prepares his doctor thesis in the field of hemodynamics of cerebral aneurysms. His research interests are CFD, analysis of the blood flow in native vessels and thrombus formation including platelet activation in flow.

Ulrich Kertzscher: He received his diploma in Physical Engineering from the Technische Universität Berlin in 1989, and his doctorate (Eng.) from the Technical University Karlsruhe in 1994. Since 1997 Ulrich Kertzscher works at the Biofluid Mechanics Laboratory, Charité - Universitätsmedizin Berlin first as research assistant and then as laboratory director. He teaches Biofluid Mechanics at the Technical University Berlin. His research interests are quantitative visualization, PIV, flow optimization of artificial organs and analysis of the blood flow in native vessels.